Analysis of defect coupling in one- and two-dimensional photonic crystals

Sheng Lan, Satoshi Nishikawa, Yoshimasa Sugimoto, Naoki Ikeda, Kiyoshi Asakawa, and Hiroshi Ishikawa
The Femtosecond Technology Research Association (FESTA), 5-5 Tokodai, Tsukuba 300-2635, Japan
(Received 14 June 2001; revised manuscript received 1 November 2001; published 5 April 2002)

Coupling of defects in one-dimensional (1D) and two-dimensional (2D) photonic crystals (PC's) is analyzed theoretically and investigated numerically using the transfer-matrix method and the finite-difference time-domain technique. Basically, the coupling behavior of defects is reflected in the spectra of PC molecules formed by two identical PC atoms (single defects). In both 1D and 2D cases, PC atoms can be roughly classified into two types based on the spectral shape of the resulting PC molecules. One type of PC atom generates clear bonding and antibonding states in the spectra of PC molecules. In contrast, the other type of PC atom creates PC molecules whose spectra are nearly flat on top. It is shown that this kind of PC atom is crucial for the construction of coupled cavity waveguides with quasiflat impurity bands. More accurately, we use a quantity related to the valley depth in the spectra of PC molecules to describe the coupling behavior of PC atoms. The dependence of this quantity on the properties of individual PC atoms is investigated in detail. It is revealed that the coupling of PC atoms is governed by the linewidth ($\delta\omega$) and the frequency shift of the PC atoms ($\Delta\omega$) upon increasing the confinement. The factor $(\Delta\omega/\delta\omega)^2$ is confirmed by theoretical analysis and numerical calculation to be a universal criterion to characterize the coupling behavior of both 1D and 2D PC defects.

DOI: 10.1103/PhysRevB.65.165208 PACS number(s): 42.70.Qs, 42.60.Da

I. INTRODUCTION

Single defects, which are intentionally created in photonic crystals (PC's),[1] have demonstrated their potential applications in the fabrication of lasers,[2] light-emitting diodes,[3,4] and filters.[5,6] Recently, the coupling of localized defect modes in PC's attracted much attention because it provides some important functions which cannot be achieved with a single defect.[7–12] Actually, it was investigated theoretically and demonstrated experimentally that waveguides made of coupled defects, which are now referred to as coupled cavity waveguides (CCW's), exhibit some advantages over conventional PC waveguides.[8,10–12] In addition, all-optical switches utilizing the band gaps formed in PC impurity bands have been proposed.[13] Moreover, it was suggested that impurity bands could be employed to build compact optical delay lines for ultrashort pulses.[14] In principle, PC impurity bands can combine the effects of wave guiding and the enhancement of nonlinearity and/or group delay. The devices described above make use of this important feature of impurity bands.

Obviously, optical waveguides, switches, and delay lines will be important components for all-optical signal processing in the future. So far, an experimental demonstration of the impurity band-based devices, e.g., CCW's and splitters, was carried out only in the microwave region.[10–12] Although the properties of impurity bands would remain unchanged due to the scaling feature of the Maxwell equations, we need to consider the interaction of impurity bands with ultrashort pulses in the optical wavelength region. This means that the transmission of ultrashort pulses with small attenuation and distortion has become the basic requirement or the first priority to be considered. Therefore, how to design impurity bands suitable for the transmission of ultrashort pulses turns out to be a crucial issue.

It is known that a single defect mode will generally split into two defect modes (bonding and antibonding states) when two identical defects (PC atoms) are coupled to form a PC molecule.[9–11] Basically, an impurity band formed by the coupling of N defect modes would normally contain N resonances in its transmission spectrum. In general, these resonances in transmittance represent the minima in group velocity.[11,14] Obviously, ripples in group velocity or group delay are undesirable, because they would distort the ultrashort pulses transmitted through the structure. From the viewpoint of design, relatively flat impurity bands are necessary in order to perfectly transmit ultrashort pulses.[14,15] To achieve this, it is necessary to investigate the coupling behavior of defects in PC's.

In this paper, we present a systematic study of the coupling of defects in one-dimensional (1D) and 2D PC's. It is organized as follows. In Sec. II, the defect structures and the investigation methods are described. Then the coupling of 1D defects is studied in Sec. III, based on the spectra of PC molecules, paying attention to PC molecules with flat spectra. In Sec. IV, the spectra of PC molecules are analytically deduced from those of PC atoms. The intrinsic mechanism for the generation of PC molecules with flat spectra is revealed, and the role of the PC atom's phase is clarified. In Sec. V, a quantity related to the valley depth in the spectra of PC molecules is used to accurately describe the coupling behavior of PC atoms. The relationship between the coupling behavior and the properties of individual PC atoms is analytically derived and numerically confirmed. Then the coupling strength and the effect of additional confinement are discussed in Sec. VI. In Sec. VII, the coupling of 2D defects is investigated. The factor that determines the coupling behavior of 2D defects is discussed and examined numerically in Sec. VIII. Finally, our findings about the coupling of defects in both 1D and 2D cases are summarized in Sec. IX.

 ©2002 The American Physical Society

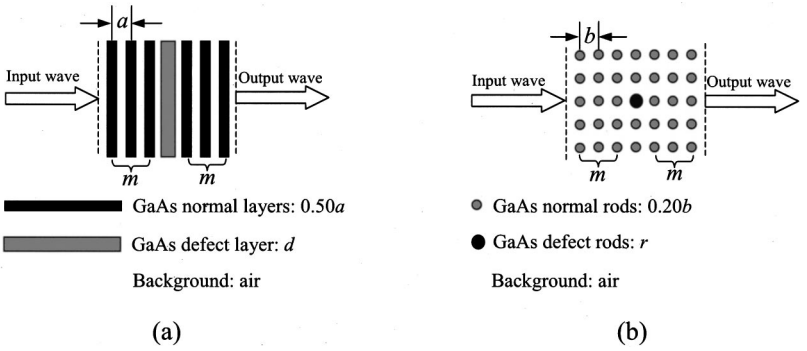

FIG. 1. (a) 1D single defect (a 1D PC atom) created in a 1D PC made of GaAs layers embedded in air. (b) 2D single defect (a 2D PC atom) created in a 2D PC made of GaAs rods embedded in air.

II. DEFECT STRUCTURES AND INVESTIGATION METHODS

Defects in both 1D and 2D PC's, formed by high-index dielectric elements embedded in a low-index background, are investigated, as schematically shown in Figs. 1(a) and 1(b). The conclusions can be easily generalized to the other type of PC's formed by low-index elements embedded in a high-index background. In the 1D case, we study a GaAs defect layer created in a 1D PC composed of GaAs ($\varepsilon_1 = 11.56$) and air ($\varepsilon_2 = 1.00$) layers with equal thickness of $0.50a$, where a is the lattice constant. In the 2D case, we consider a 2D PC formed by GaAs rods of infinite length arranged in a square lattice. The radius of GaAs rods is $0.20b$, where b is the lattice constant. By modifying the radius of the central GaAs rod to r, defects are created in the 2D PC.

For the study of 1D PC structures, it is convenient to use the transfer-matrix method introduced by Pendry and MacKinnon, because both the amplitude and phase information of the complex transmission coefficient can be simultaneously obtained.[16] In the 2D case, however, it is necessary to build identical supercells whose size is large enough to ensure the isolation between them in order to obtain information about a single defect. As an alternative, we turn to the finite-difference time-domain method proposed by Yee.[17] With this technique, it is easy to achieve the transmission spectrum as well as the field distribution for a 2D PC structure.

III. 1D DEFECTS AND THEIR COUPLING

By changing the size of a defect, the resonant frequency of the defect can be tuned within the band gap, as shown in Fig. 2 for the 1D defect. It is noted, however, that the defect position (or resonant frequency) generally exhibits to some extent a dependence on the confinement of electromagnetic field within the defect region which is determined by the number of normal elements on both sides of the defect (m). The examples of strong and weak dependences, which are given by defect sizes (d) of $0.30a$ and $0.00a$ respectively, are illustrated in Figs. 3(a) and 3(b) together with the phase information. Here the phase $\varphi(\omega)$ is defined in the complex transmission coefficient $t(\omega) = T^{1/2}(\omega)e^{i\varphi(\omega)}$ as that accumulated by the field on transmission relative to the phase (zero) of the incident field. It is found that the phase at the transmission peak is close to zero for the $0.30a$ defect, while it is nearly $\pm\pi/2$ for the $0.00a$ defect. With increasing confinement (or increasing m), the phase of the transmission peak is barely changed in both cases. However, it can be seen in Fig. 3(a) that for the $0.30a$ defect the separation between the transmission peak and the frequency where the phase is $\pm\pi/2$ becomes smaller, and finally approaches zero for infinitely strong confinement. In sharp contract, for the $0.00a$ defect, the transmission peak as well as the frequency where the phase is $\pm\pi/2$ is almost insensitive to the confinement, as shown in Fig. 3(b).

Basically, the coupling behavior of PC defects (PC atoms) is reflected in the spectra of the resulting PC molecules. In Fig. 4, we show the transmission spectra of the PC molecules formed by the coupling of two PC atoms given in Fig. 3(a) with different confinement strengths ($m = 2$ and 4). Phase information about the constituting PC atoms is also provided. Obviously, we can see clearly the so-called bonding and antibonding states. Their splitting characterizes the coupling strength between the two PC atoms. With increasing confinement or defect separation, the coupling strength is reduced. It is manifested as a reduction in the splitting. However, it is important to note that the bonding state appears at the same position as the transmission peak of the PC atom while the antibonding state appears at the frequency where the phase of the individual PC atoms is $\pm\pi/2$. It is also remarkable that the reduction of the splitting is always accompanied by a narrowing of the linewidth for the bonding and antibonding states. Consequently, the valley at the center of the spectra for PC molecules remains, and it becomes even deeper for strong confinement.

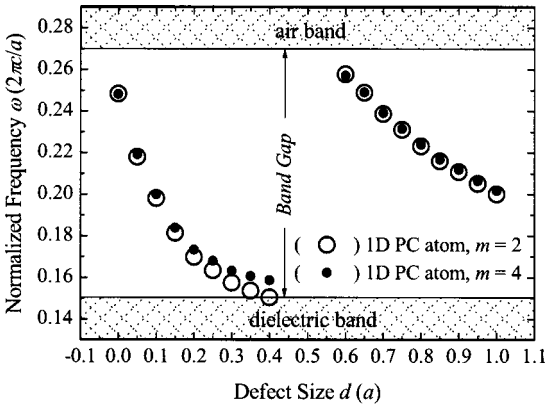

FIG. 2. Dependence of resonant frequency on defect size in 1D PC atoms with different confinement strengths ($m = 2$ and 4).

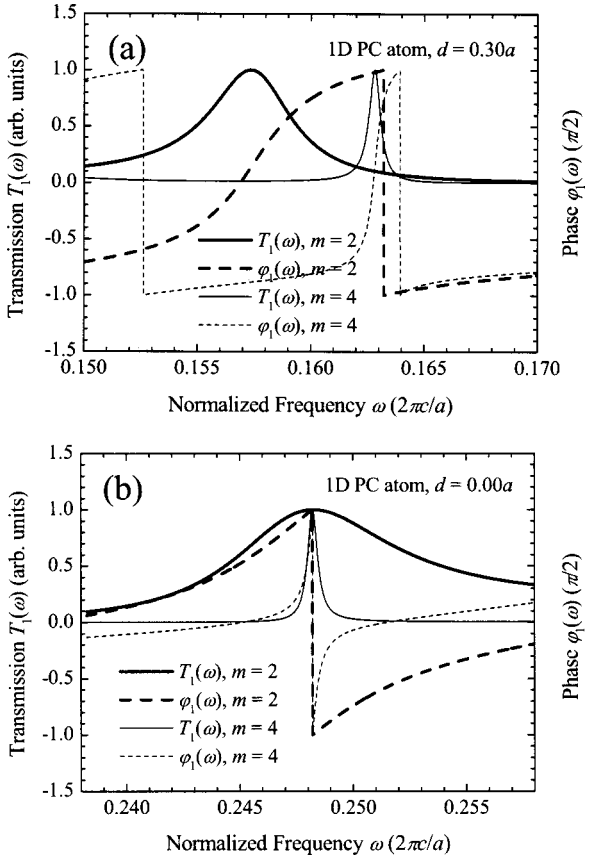

FIG. 3. Transmission and phase spectra for PC atoms of different confinement strengths ($m=2$ and 4) with defect sizes of (a) $d=0.30a$ and (b) $d=0.00a$.

The transmission spectra of several typical PC molecules formed by PC atoms ($m=2$) located at different positions in the band gap are shown in Figs. 5(a)–5(c). The spectra of the constituting PC atoms are also provided for comparison. Surprisingly, we cannot distinguish between bonding and antibonding states in some PC molecules (e.g., the $d=0.00a$ defect). Instead, only a flat region with nearly unit transmission is observed in the spectra of these PC molecules. As compared to the spectra of the constituting PC atoms, the region with unit transmission is significantly widened, while the linewidth is slightly narrowed.

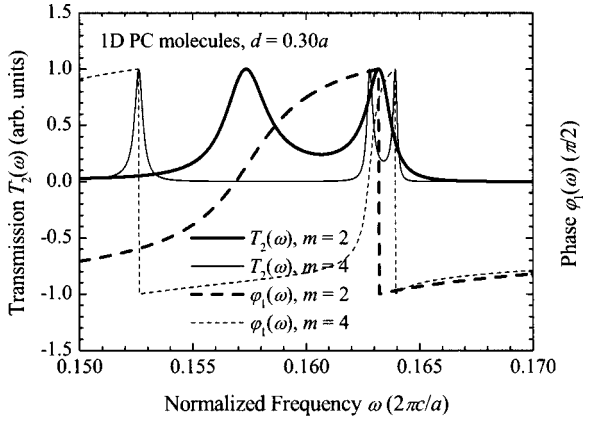

FIG. 4. Transmission spectra of the PC molecules and the phase spectra of the constituting PC atoms ($d=0.30a$) for two different confinement strengths ($m=2$ and 4). The left peak in $T_2(\omega)$ ($m=4$) is the outermost resonance in the pass band (dielectric band).

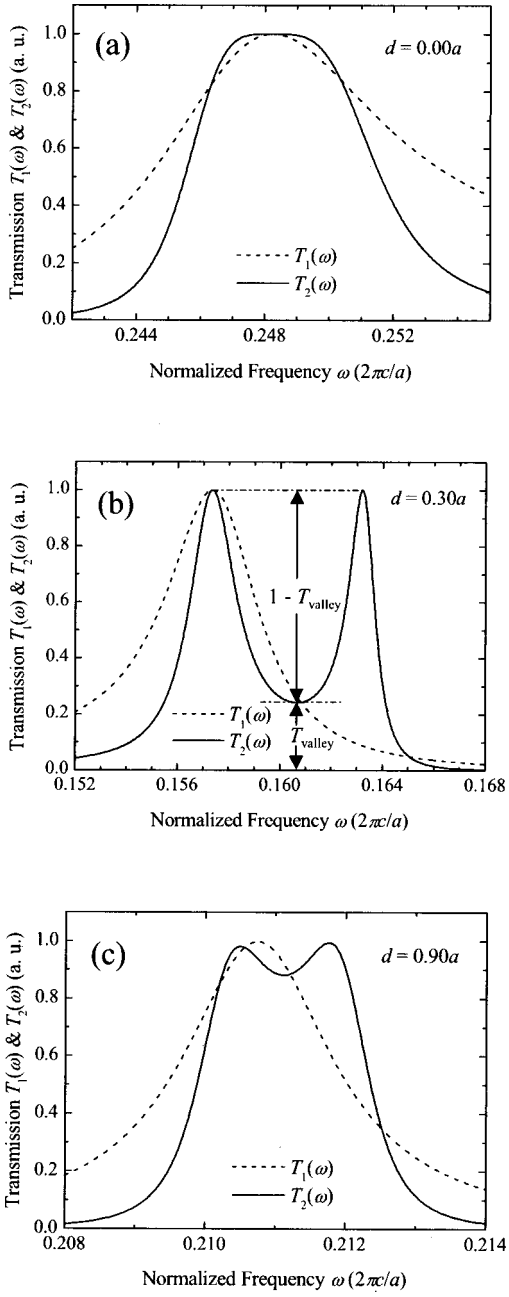

FIG. 5. Transmission spectra of 1D PC molecules (solid curves) formed by different PC atoms (dashed curves). (a) $d=0.00a$, (b) $d=0.30a$, (c) $d=0.90a$.

Now we examine the transmission spectra of the impurity bands formed with two types of PC atoms, namely, those generating bonding and antibonding states in PC molecules (type A) and those creating only a flat region in PC molecules (type B). Two typical cases in which the defect sizes are $0.30a$ and $0.00a$ are presented in Figs. 6(a) and 6(b) for comparison. It can be seen that strong resonances in transmittance appear in the former while a quasiflat impurity band

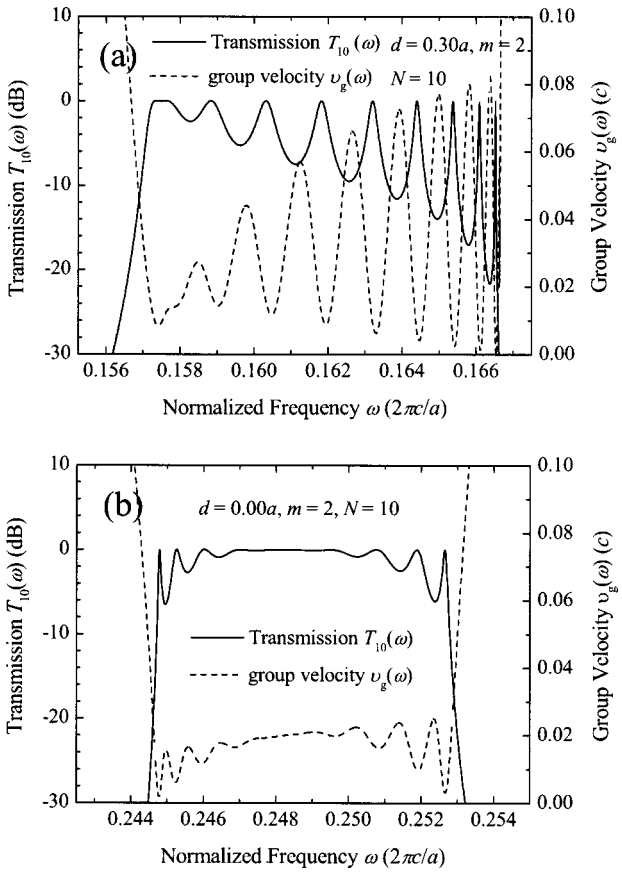

FIG. 6. Transmission and group velocity spectra for the impurity bands formed by ten PC atoms ($m=2$) with a defect size of (a) $d=0.30a$ and (b) $d=0.00a$.

is obtained in the latter. Also, the group velocity for the nonflat and quasiflat impurity bands is calculated. We can easily find that the resonances in transmittance correspond to the ripples in group velocity. The stronger the former, the larger the latter. In order to transmit ultrashort pulses without introducing serious attenuation and distortion, a quasiflat impurity band, such as shown in Fig. 6(b), is highly desirable.[14,15]

IV. SPECTRA OF PC MOLECULES DEDUCED FROM THOSE OF PC ATOMS

The research work of Dowling and co-workers allows us to deduce the spectra of PC molecules and even PC solids from those of PC atoms, at least in the 1D case.[18,19] Basically, they have investigated how to derive the amplitude and phase of the complex transmission coefficient for a periodic structure once the information about a unit cell is known. Specifically, it is indicated that these expressions are independent of the content of the unit cell, i.e., they are valid for an arbitrary distribution of refractive index in the unit cell. No doubt, these formulas can be employed to extract the spectra of PC molecules from those of PC atoms. The intrinsic mechanism for the formation of different types of PC molecules may become evident if we analytically extract the spectra of PC molecules using these formulas.

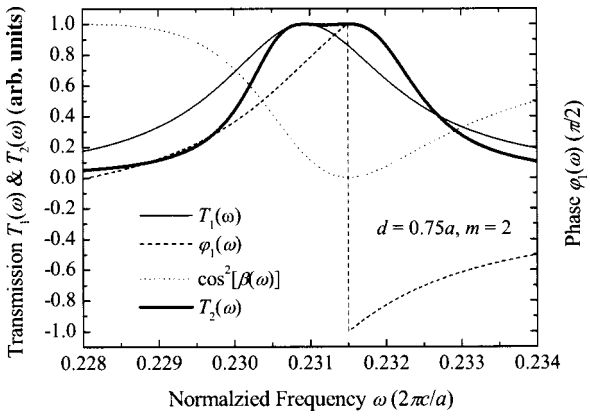

FIG. 7. Transmission spectrum of the 1D PC molecule deduced by that of a PC atom ($m=2$) with a defect size of $0.75a$.

Generally, the transmission spectrum of a periodic structure composed of N unit cells is given by[18,19]

$$T_N(\omega)=\frac{1}{1+\left[\frac{1}{T_1(\omega)}-1\right]\frac{\sin^2[N\beta(\omega)]}{\sin^2[\beta(\omega)]}}, \tag{1}$$

where $T_N(\omega)$ and $T_1(\omega)$ are the transmission spectra of the periodic structure and the unit cell, respectively. Here $\beta(\omega)$ is the Bloch phase for the hypothetical infinite periodic structure. It is related to the phase of the complex transmission coefficient $\varphi_1(\omega)$ by[18,19]

$$\cos[\beta(\omega)]=\mathrm{Re}\left\{\frac{1}{t_1(\omega)}\right\}=\frac{1}{\sqrt{T_1(\omega)}}\cos[\varphi_1(\omega)]. \tag{2}$$

Applying these formulas to PC molecules, we obtain the relationship between the spectra of PC molecules $[T_2(\omega)]$ and PC atoms $[T_1(\omega)]$:

$$\begin{aligned}T_2(\omega)&=\frac{1}{1+4[1-T_1(\omega)]\cos^2[\beta(\omega)]}\\&=\frac{1}{1+4\dfrac{[1-T_1(\omega)]}{T_1(\omega)}\cos^2[\varphi_1(\omega)]}.\end{aligned} \tag{3}$$

From this it is apparent that the transmission is maximum (unity) at least for two points which represent the transmission peaks for the bonding and antibonding states. One is at the transmission peak of the PC atom $[T_1(\omega)=1]$ and the other appears at the frequency where the phase of the PC atom is $\pm\pi/2$ $(\cos[\varphi_1(\omega)]=\cos[\beta(\omega)]=0)$. In between these two points, if the second term in the denominator of $T_2(\omega)$ is rather small, then $T_2(\omega)$ is very close to unity, forming a flat region. To illustrate the generation of type-B PC molecules, in Fig. 7 we show the transmission and phase spectra of a PC atom, the corresponding $\cos[\beta(\omega)]$, and the transmission spectrum of the resulting PC molecule, using $0.75a$ defect as an example. From this it is understandable why the antibonding state always appears at the frequency where the phase of the PC atom is equal to $\pm\pi/2$. Also, it becomes clear that

bonding and antibonding states appear in type-A PC molecules whose constituting PC atoms have a phase close to zero at the transmission peak. For type-B PC molecules, formed by PC atoms whose phase at the transmission peak is close to $\pm\pi/2$, a flat region is created.

V. FACTOR DETERMINING THE COUPLING BEHAVIOR OF 1D DEFECTS

Actually, the relationship between the coupling behavior and the transmission phase of PC atoms derived above is only a rule of thumb. As can be seen in Fig. 5, there is no strict boundary between the type-A and -B atoms. Sometimes, only a small dip appears at the center of the spectra for PC molecules. In these cases, it is hard to classify the PC atoms as type A or B (e.g., $d=0.90a$). Strictly speaking, we need to use another quantity to accurately describe the coupling behavior of PC atoms. Apparently, it is the depth of the valley in the spectra of the resulting PC molecules which is defined as follows:

$$D_{\text{valley}}=\frac{T_{\text{peak}}-T_{\text{valley}}}{T_{\text{peak}}}. \tag{4}$$

In the case when only the spectral shape is considered, we can always normalize the transmission spectra and simplify Eq. (4) as

$$D_{\text{valley}}=1-T_{\text{valley}}. \tag{5}$$

However, it will be shown later that it is more convenient to use another quantity R_{valley}, for the description of the coupling behavior, which is defined as

$$R_{\text{valley}}=\frac{1-T_{\text{valley}}}{T_{\text{valley}}}. \tag{6}$$

Obviously, R_{valley} is the ratio of the valley depth to the transmission at the bottom of the valley, as indicated in Fig. 5(b). Thus it can be used to characterize the coupling behavior of PC atoms.

Now it is necessary to understand what governs the value of R_{valley}. To answer this question, we have to go back to Eq. (3), from which we can extract the spectra of PC molecules from those of PC atoms. We simply rewrite the formula as

$$T_2(\omega)=\frac{1}{1+F(\omega)}, \tag{7}$$

$$F(\omega)=4\frac{[1-T_1(\omega)]}{T_1(\omega)}\cos^2[\varphi_1(\omega)]. \tag{8}$$

From these expressions, it is clear that $F(\omega)$ has two minimum values of zero, which correspond to the two peaks in $T_2(\omega)$, when $T_1(\omega)=1$ or $\varphi_1(\omega)=\pm\pi/2$. Between the two peaks, $T_2(\omega)$ has a minimum value T_{valley}, corresponding to the bottom of the valley. This is determined by the maximum value of $F(\omega)$:

$$T_{\text{valley}}=\frac{1}{1+F_{\max}(\omega)}. \tag{9}$$

From this, it is readily apparent that

$$F_{\max}(\omega)=\frac{1-T_{\text{valley}}}{T_{\text{valley}}}=R_{\text{valley}} \tag{10}$$

This means that the coupling behavior is completely determined by the maximum value of $F(\omega)$. Thus it is clear why it is more convenient to use R_{valley} rather than D_{valley} to describe the coupling behavior of PC atoms. What we need to do is to find the dependence of $F_{\max}(\omega)$ on the properties of individual PC atoms.

From $F'(\omega)=0$, we obtain the following equation:

$$[T_1(\omega)-T_1^2(\omega)]\sin[2\varphi_1(\omega)]\varphi_1'(\omega)+T_1'(\omega)\cos^2[\varphi_1(\omega)]=0. \tag{11}$$

For simplicity, we consider PC atoms whose resonant frequency shifts to the high-frequency side as the confinement increases. PC atoms whose resonant frequency shifts to the low-frequency side can be treated very similarly. More concretely, we assume that the peak of $T_1(\omega)$ appears at ω_0 while the $\pm\pi/2$ phase shift is obtained at ω_1. In addition, we define two quantities which are believed to reflect the characteristics of PC atoms. One is the normalized frequency shift $\Delta\omega/\omega_0=|\omega_{m\to\infty}-\omega_0|/\omega_0$, and the other is the Q factor of the defect modes which is defined as $Q=\omega_0/\delta\omega$, where $\delta\omega$ is the linewidth of $T_1(\omega)$. Since the separation between the transmission peak and the frequency where the transmission phase is $\pi/2$ (ω_1) becomes smaller with increasing confinement and finally approaches zero for infinitely strong confinement (as shown in Fig. 3(a)), we have $\Delta\omega/\omega_0=|\omega_{m\to\infty}-\omega_0|/\omega_0\approx|\omega_1-\omega_0|/\omega_0$. Further, we know that $T_1(\omega)$ and $\varphi_1(\omega)$ satisfy the following conditions:

$$0\leqslant T_1(\omega)\leqslant 1,\quad T_1(\omega_0)=1,\quad T_1'(\omega_0)=0, \tag{12a}$$

$$-\frac{\pi}{2}\leqslant\varphi_1(\omega)\leqslant\frac{\pi}{2},\quad \varphi_1(\omega_1)=\pm\frac{\pi}{2},\quad \varphi_1''(\omega_0)=0. \tag{12b}$$

Based on these conditions, it is obvious that ω_0 and ω_1 are the two solutions of Eq. (11). If we assume that ω_2 is the frequency where $F(\omega)$ is maximum, it must fulfill Eq. (11). Substituting Eq. (11) into Eq. (8), we obtain the maximum value of $F(\omega)$ as

$$F_{\max}(\omega)=-4\frac{[1-T_1(\omega)]^2}{T_1'(\omega)}\sin[2\varphi_1(\omega)]\varphi_1'(\omega). \tag{13}$$

In Eq. (13), for simplicity, we have replaced ω_2 with ω. In order to compare different defects, it is convenient to normalize the spectra of each defect mode (including the transmission and phase spectra) with its central frequency (ω_0). Consequently, the frequency shift ($\Delta\omega$) and linewidth ($\delta\omega$) discussed in the following are actually the normalized frequency shift ($\Delta\omega/\omega_0$) and the normalized linewidth ($\delta\omega/\omega_0=1/Q$), both being dimensionless quantities. In addition, we must keep in mind in the following discussion on $F_{\max}(\omega)$ that ω (now dimensionless) is in the region [1,1

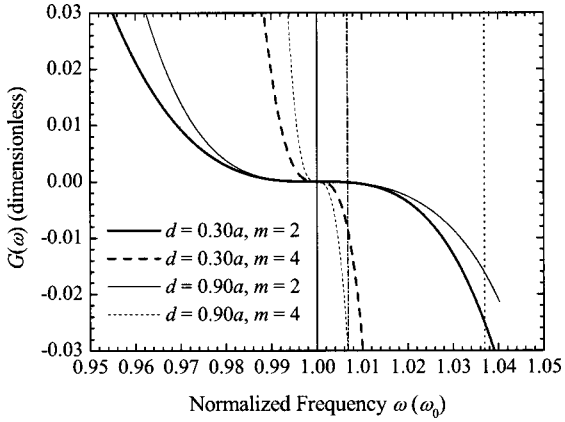

FIG. 8. Dependence of $G(\omega)(=[1-T_1(\omega)]^2/T_1'(\omega))$ on the normalized frequency shift $\Delta\omega/\omega_0$ for two different defect modes ($d=0.30a$ and $0.90a$) and different confinement strengths ($m=2$ and 4). The normalized frequency shifts ($\Delta\omega/\omega_0$) for the $d=0.30a$ defect are indicated by the dotted line ($m=2$) and the dotted-dashed line ($m=4$).

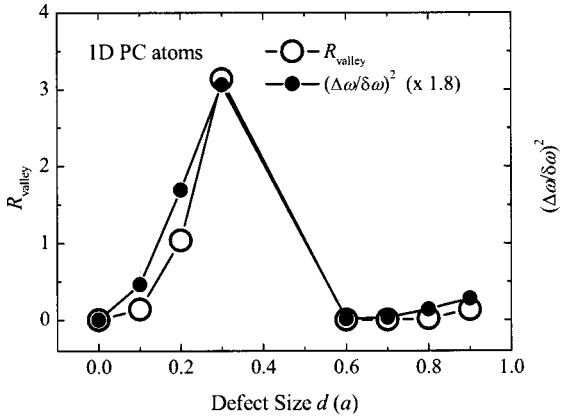

FIG. 9. Dependence of R_{valley} and $(\Delta\omega/\delta\omega)^2$ on defect size in 1D PC defects.

$+\Delta\omega]$ or $[1-\Delta\omega,1]$, depending on the direction of the frequency shift with increasing confinement.

At first glance, $F_{\max}(\omega)$ is a very complicated function. However, a careful inspection reveals that $\varphi_1'(\omega)$ is actually the group delay time provided by a defect at a frequency of ω.[19] At the central frequency ($\omega_0=1$), it reaches a maximum value [i.e., $\varphi_1''(\omega_0)=0$], which is inversely proportional to the linewidth of the defect mode, i.e., $\varphi_1'(\omega_0) \propto 1/\delta\omega$.[11] Thus $\varphi_1'(\omega)$ is inversely proportional to both the linewidth and frequency shift of the defect mode, i.e., $\varphi_1'(\omega)\propto(1/\delta\omega)\times(1/\Delta\omega)$. In addition, we know that $\Delta\omega$ is small when $\varphi_1(\omega_0)$ is close to $\pm\pi/2$ and it is large when $\varphi_1(\omega_0)$ is close to 0. Since ω is approximately at the center of the interval $[1,1+\Delta\omega]$ or $[1-\Delta\omega,1]$, $|\sin[2\varphi_1(\omega)]|\to 0$ [i.e., $2\varphi_1(\omega)\to\pm\pi$] when $\Delta\omega$ is small and $|\sin[2\varphi_1(\omega)]| \to 1$ [i.e., $2\varphi_1(\omega)\to\pm\pi/2$] when $\Delta\omega$ is large. Therefore, we find that for different defects $|\sin[2\varphi_1(\omega)]|$ is proportional to the frequency shift, i.e., $|\sin[2\varphi_1(\omega)]|\propto\Delta\omega$. However, it is noted in Fig. 3 that for the same defect, $\varphi_1(\omega_0)$ does not change with increasing confinement. Therefore, it is apparent that for the same defect $|\sin[2\varphi_1(\omega)]|$ is independent of the Q factor of defect modes. Considering the decrease of both $\Delta\omega$ and $\delta\omega$ with increasing confinement strength, it is expected that $|\sin[2\varphi_1(\omega)]|\propto\Delta\omega/\delta\omega$.

The relationship between the first term of $F_{\max}(\omega)$ ($[1-T_1(\omega)]^2/T_1'(\omega)$, denoted as $G(\omega)$ in the following) and the properties of PC atoms ($\Delta\omega$ and $\delta\omega$) is not so obvious. Thus we rely on the numerical calculation to obtain an estimate. In Fig. 8, we show the value of $G(\omega)$ calculated for two different defect modes with different confinement strengths. From Fig. 8, it can be seen that the curves of $G(\omega)$ for different defect modes are very similar. Only a dependence on the confinement strength (or Q factor) is observed. More importantly, $|G(\omega)|$ is approximately a quadratic function of $\Delta\omega$, i.e., $|G(\omega)|\propto(\Delta\omega)^2$. For a $d=0.90a$ defect whose $\Delta\omega$ is close to zero, $|G(\omega)|$ is close to zero. In contrast, $|G(\omega)|$ is large for a $d=0.30a$ defect because of its large $\Delta\omega$. If we inspect the same defect ($d=0.30a$) with different confinement strengths, it is found that $|G(\omega)|$ decreases with increasing confinement strength. However, if we note that $\Delta\omega$ becomes smaller with increasing confinement strength, the dependence of $|G(\omega)|$ on the confinement strength can be solely attributed to the change of $\Delta\omega$. This in turn confirms that $|G(\omega)|$ is proportional to $(\Delta\omega)^2$.

Summarizing the conclusions deduced from the above discussion, we obtain the relationship between the coupling behavior, which is characterized by R_{valley}, and the properties of individual PC atoms which are reflected by $\Delta\omega$ and $\delta\omega$:

$$R_{\text{valley}}\propto(\Delta\omega)^2\left(\frac{\Delta\omega}{\delta\omega}\right)\left(\frac{1}{\delta\omega}\frac{1}{\Delta\omega}\right)=\left(\frac{\Delta\omega}{\delta\omega}\right)^2. \qquad (14)$$

This expression indicates that the coupling of PC atoms is basically governed by the frequency shift with increasing confinement and the linewidth of PC atoms.

In order to verify this, we have numerically calculated R_{valley} and $(\Delta\omega/\delta\omega)^2$ for different 1D PC defects and plotted them as a function of defect size in Fig. 9. An exact correspondence between R_{valley} and $(\Delta\omega/\delta\omega)^2$ can be found, confirming the validity of our analysis presented above.

VI. COUPLING STRENGTH AND ADDITIONAL CONFINEMENT

It is necessary to clarify two issues that may cause some confusion. First, the appearance of type-B PC molecules with flat transmission regions is not due to the weak-coupling strength. It originates from the nature of PC atoms which is characterized by $(\Delta\omega/\delta\omega)^2$. Basically, the coupling strength is determined by the overlap of the fields in the two PC atoms. Therefore, it should be dependent on the Q factor of the PC atoms.

In Fig. 4, we see the reduction of coupling strength in type-A PC atoms with increasing confinement or Q factor. It is obvious that the reduction of coupling strength does not lead to the merger of bonding and antibonding states or to a flat region. The coupling strength is inversely proportional to the Q factor of PC atoms, and it has nothing to do with the type of PC atoms.

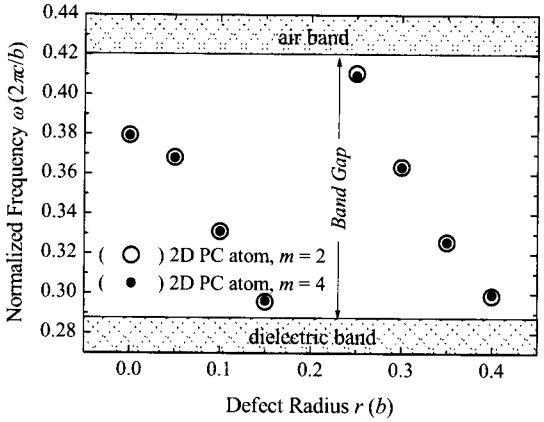

FIG. 10. Dependence of resonant frequency on defect size in 2D PC atoms with different confinement strengths ($m=2$ and 4).

Second, bonding and antibonding states can be resolved if we add additional confinement on both sides of type-B PC molecules. This is the case when two defects are generated deeply in a PC.[10,11] When an additional confinement is added, the PC structure can not be divided into PC atoms with symmetric confinement. It means that the formulas given in Eqs. (1) and (3) are no longer appropriate for describing the transmission properties of the PC structure. In this paper, we investigated the dependence of the transmission properties of PC molecules and PC solids on the properties of the constituting PC atoms. In order words, the PC molecules and PC solids we studied here are constructed by the periodic repetition of PC atoms (unit cells). This implies that the number of normal elements on each side of the PC structures is always the half of the number of normal elements in between two defects which is an even number. Actually, this is the basic condition to achieve quasiflat impurity bands in CCW's.[14] Indeed, the availability of quasiflat impurity bands depends not only on the intrinsic properties of PC defects studied in this paper but also on the configuration of CCW's.[14] The additional confinement plays a role similar to a Fabry-Perot cavity in selecting the cavity mode from a continuum (the flat region).

VII. 2D DEFECTS AND THEIR COUPLING

The relationship between the resonant frequency and defect size for the 2D defects we studied is given in Fig. 10 for two different confinement strengths ($m=2$ and 4). Here only the single and doubly degenerate defect modes generated by $r/b<0.42$ are considered. Obviously, nearly all of the defect modes exhibit a much weaker dependence of resonant frequency on confinement strength as compared to the 1D case. It should be emphasized that the confinement in the transverse direction (perpendicular to the transmitting direction) does not affect the resonant frequencies of the defect modes if it is strong enough. Thus the number of normal elements on both sides of the defect along this direction is chosen to be 7 in our 2D defects.

The spectra of several PC atoms ($m=2$) and the resulting PC molecules versus defect size are shown in Figs. 11(a)–11(c). Since we are concerned only about the spectral shape,

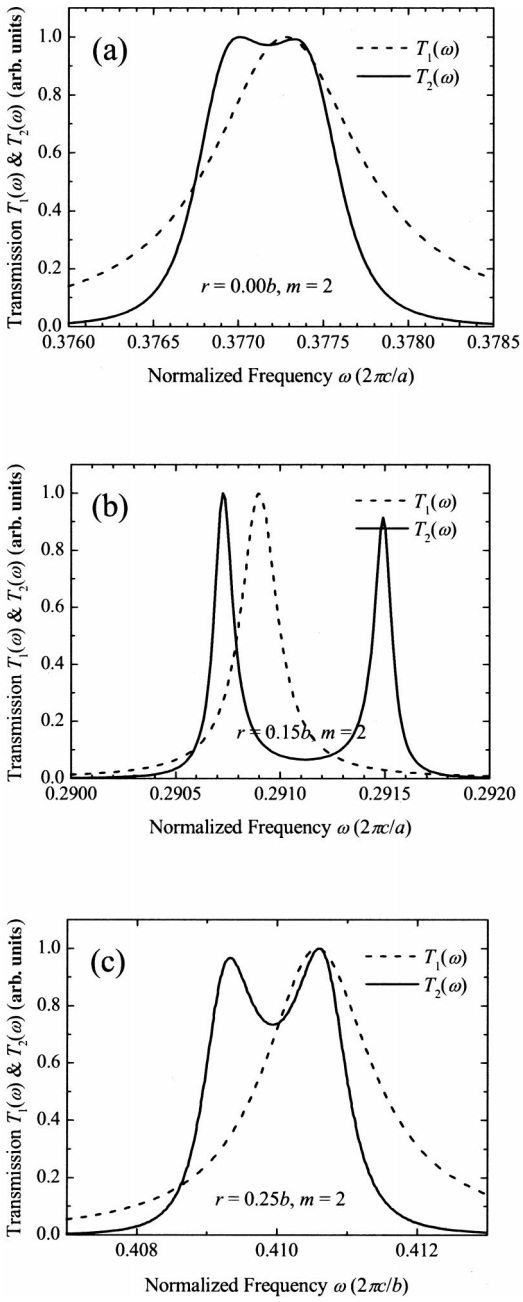

FIG. 11. Transmission spectra of 2D PC molecules (solid curves) formed by different PC atoms (dashed curves). (a) $r=0.00b$, (b) $r=0.15b$, (c) $r=0.25b$.

all of the spectra have been normalized to unity. Obviously, both type-A and -B PC molecules are observed. Unfortunately, it is difficult to extend the formulas derived by Dowling and co-workers to 2D case because of two reasons. First the transmission in the 2D case depends strongly on the mode matching between the input field (e.g., the shape and spatial width) and the defect mode. Second, we need to place the detector just after the PC atoms ($b/2$ from the final row of the elements) to obtain the correct transmission phase. However, the electric field there is usually enhanced to some extent, especially for PC atoms with large Q factors. Therefore, it is difficult to accurately determine $T_1(\omega)$ and $\varphi_1(\omega)$ for 2D defects.

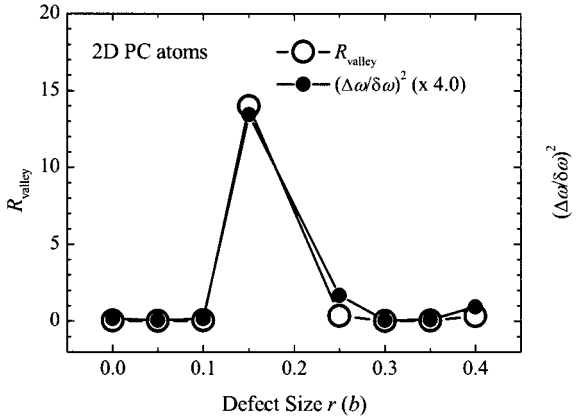

FIG. 12. Dependence of R_{valley} and $(\Delta\omega/\delta\omega)^2$ on defect size in 2D PC defects.

In the 1D defects studied here, it appears that type-A PC molecules are available for the PC atoms located on the low-energy side of the gap center. On the other hand, the PC atoms located on the high-energy side are favorable for the formation of type-B PC molecules. It is known that the electromagnetic field is concentrated in the defect layer for PC atoms close to the dielectric band, while it is mainly distributed in the two neighboring air layers for PC atoms near the air band. Therefore, it is suspected that the pattern of the field distribution within the defect region may determine the coupling behavior of the defects in 2D PCs.

In the 2D case, the defect mode appears as monopole for $0.00 \leqslant r/b < 0.20$. For $0.20 < r/b < 0.42$, we have doubly degenerate modes whose field distribution is a dipole.[20] In other words, these two types of distributions are completely different. Although most of the PC molecules formed by PC atoms located on the high-energy side appear as type B, it is found that the PC molecule formed by $r/b = 0.25$ PC atom is type A. This exception indicates that the coupling behavior does not rely on the distribution of electric field within the defects.

VIII. FACTOR DETERMINING THE COUPLING BEHAVIOR OF 2D DEFECTS

In most practical cases, the confinement perpendicular to the propagation direction in 2D CCW's is sufficiently strong and the coupling of 2D defects are expected to be very similar to that of 1D defects. Although Eqs. (1) and (3) may not be perfectly extended to the 2D case, a qualitative analysis of the coupling behavior of 2D defects is still possible by using Eq. (3). It is noted that there are no special requirements for structure to derive the relationship between R_{valley} and the properties of individual PC atoms [Eq. (14)] from Eq. (3). Similarly, a shift of the transmission peak is also commonly observed in 2D PC defects although is relatively small. Therefore, we expect that the value of R_{valley} in the 2D case could still be determined by $(\Delta\omega/\delta\omega)^2$.

In order to confirm this, we have computed the values of R_{valley} and $(\Delta\omega/\delta\omega)^2$ for the 2D defects we studied, and they are plotted in Fig. 12 for comparison. Since the frequency shift decreases exponentially with increasing confinement strength (increasing m), we have used $|\omega_{m=4} - \omega_{m=2}|$ to approximate $|\omega_{m=\infty} - \omega_{m=2}| = \Delta\omega$. Clearly, R_{valley} and $(\Delta\omega/\delta\omega)^2$ exhibit nearly the same dependence on the defect size. It confirms that the coupling behavior of 2D defects is still governed by $(\Delta\omega/\delta\omega)^2$.

Before summarizing, we want to address the two important issues which are closely related to the coupling of PC defects investigated in this work. First, like the Q factor of PC defects, the normalized frequency shift is another very important feature of PC defects which reflects the response or sensitivity of the PC defects to the confinement strength. It is known that the transmission coefficient is a complex containing the information of amplitude and phase. By looking at Eqs. (1)–(3), it is apparent that the transmission phase plays an important role in determining the coupling behavior of PC defects. The Q factor gives the only information about amplitude, and it determines the coupling strength of PC defects. In order to obtain the spectral shape of PC molecules and PC solids, it is necessary to find out the transmission phase of the constituting PC atoms. It has been shown that the shift of defect modes upon the increase of confinement (i.e., the sensitivity of the defect modes) depends strongly on the phase of the defect modes. Thus the normalized frequency shift is a physical quantity that contains the information of transmission phase. It can be either theoretically calculated or experimentally measured, just like the Q factor of PC defects. In the case when the calculation or measurement of transmission phase is not convenient, it is possible to obtain information about the transmission phase through a characterization of a normalized frequency shift which belongs to the characterization of transmission amplitude.

Second, it must be emphasized that the coupling discussed in this paper is the coupling of PC defects (atoms). It is necessary to distinguish it form the coupling between a PC structure and an incident field, although they are closely related. Certainly, the transmission properties of a PC atom generally depend on the incident field. However, our finding makes it possible to predict the major features in the transmission spectrum of a PC solid (or a CCW) once the transmission properties of the constituting PC atoms are known. Therefore, the dependence of the transmission properties of the PC solid on a certain incident field is indirectly involved through the response of the constituting PC atoms to the same incident field.

IX. CONCLUSION

In summary, we have investigated the coupling behavior of defects in 1D and 2D PCs. The coupling behavior is basically reflected in the spectra of PC molecules formed by two PC atoms (single defects). It does not depend on the field distribution within the defects. Instead, it is governed by the Q factor and the normalized frequency shift of the PC atoms upon the increase of confinement. In the 1D case, as a rule of thumb, the coupling behavior of PC atoms is determined by their transmission phases. For PC atoms whose transmission phase is close to zero, the spectra of PC molecules are composed of clear bonding and antibonding states. In contrast, the spectra of PC molecules formed by PC atoms

whose transmission phase is close $\pm\pi/2$ are flat on top. More accurately, we use a quantity which is related to the valley depth in the spectra of the resulting PC molecules to describe the coupling behavior of PC atoms. It is proportional to the square of the ratio of the frequency shift to the linewidth of the PC atoms. The factor $(\Delta\omega/\delta\omega)^2$ is confirmed by theoretical analysis and numerical calculation to be a universal quantity to characterize the coupling of both 1D and 2D PC defects. Furthermore, it is shown that the PC atoms generating PC molecules with flat spectra are important for the construction of CCW's with quasiflat impurity bands suitable for the transmission of ultrashort pulses.

ACKNOWLEDGMENT

This work was supported by the New Energy and Industrial Technology Development Organization (NEDO) within the framework of the Femtosecond Technology Project.

[1] E. Yablonovitch, T. J. Gmitter, R. D. Meade, A. M. Rappe, K. D. Brommer, and J. D. Joannopoulos, Phys. Rev. Lett. **67**, 3380 (1991).
[2] O. Painter, R. K. Lee, A. Scherer, A. Yariv, J. D. O'Brien, P. D. Dapkus, and I. Kim, Science **284**, 1819 (1999).
[3] S. Fan, P. R. Villeneuve, J. D. Joannopoulos, and E. F. Schubert, Phys. Rev. Lett. **78**, 3294 (1997).
[4] M. Boroditsky, T. F. Krauss, R. Coccioli, R. Vrijen, R. Bhat, and E. Yablonovitch, Appl. Phys. Lett. **75**, 1036 (1999).
[5] S. Fan, P. R. Villeneuve, J. D. Joannopoulos, and H. A. Haus, Phys. Rev. Lett. **80**, 960 (1996).
[6] S. Noda, A. Chutinan, and M. Imada, Nature (London) **407**, 608 (2000).
[7] E. Lidorikis, M. M. Sigalas, E. N. Economou, and C. M. Soukoulis, Phys. Rev. Lett. **81**, 1405 (1998).
[8] A. Yariv, Y. Xu, R. K. Lee, and A. Scherer, Opt. Lett. **24**, 711 (1999).
[9] M. Bayer, T. Gutbrod, A. Forchel, T. L. Reinecke, P. A. Knipp, R. Werner, and J. P. Reithmaier, Phys. Rev. Lett. **83**, 5374 (1999).
[10] M. Bayindir, B. Temelkuran, and E. Ozbay, Phys. Rev. Lett. **84**, 2140 (2000); Phys. Rev. B **61**, R11855 (2000); Appl. Phys. Lett. **77**, 3902 (2000).
[11] M. Bayindir and E. Ozbay, Phys. Rev. B **62**, R2247 (2000).
[12] M. Bayindir, E. Ozbay, B. Temelkuran, M. M. Sigalas, C. M. Soukoulis, R. Biswas, and K. M. Ho, Phys. Rev. B **63**, 081107 (2001).
[13] S. Lan, S. Nishikawa, and O. Wada, Appl. Phys. Lett. **78**, 2101 (2001).
[14] S. Lan, S. Nishikawa, Hiroshi Ishikawa, and O. Wada, J. Appl. Phys. **90**, 4321 (2001).
[15] G. Lenz, B. J. Eggleton, C. K. Madsen, and R. E. Slusher, IEEE J. Quantum Electron. **37**, 525 (2001).
[16] J. B. Pendry and A. MacKinnon, Phys. Rev. Lett. **69**, 2772 (1992).
[17] K. S. Yee, IEEE Trans. Antennas Propag. **AP-14**, 302 (1966).
[18] J. M. Bendickson, J. P. Dowling, and M. Scalora, Phys. Rev. E **53**, 4107 (1996).
[19] J. P. Dowling, IEE Proc.: Optoelectron. **145**, 420 (1998).
[20] P. R. Villeneuve, S. Fan, and J. D. Joannopoulos, Phys. Rev. B **54**, 7837 (1996).